Optogenetic control of chemokine receptor signal and T-cell migration

Yuexin Xu[a,b,1], Young-Min Hyun[a,b,1], Kihong Lim[b], Hyunwook Lee[b], Ryan J. Cummings[a], Scott A. Gerber[a], Seyeon Bae[b], Thomas Yoonsang Cho[c], Edith M. Lord[a], and Minsoo Kim[a,b,2]

[a]Department of Microbiology and Immunology and [b]David H. Smith Center for Vaccine Biology and Immunology, University of Rochester, Rochester, NY 14642; and [c]Edward A. Doisy Department of Biochemistry and Molecular Biology, Saint Louis University School of Medicine, Saint Louis, MO 63104

Edited by Jason G. Cyster, University of California, San Francisco, CA, and accepted by the Editorial Board March 17, 2014 (received for review October 15, 2013)

Adoptive cell transfer of ex vivo-generated immune-promoting or tolerogenic T cells to either enhance immunity or promote tolerance in patients has been used with some success. However, effective trafficking of the transferred cells to the target tissue sites is the main barrier to achieving successful clinical outcomes. Here we developed a strategy for optically controlling T-cell trafficking using a photoactivatable (PA) chemokine receptor. Photoactivatable-chemokine C-X-C motif receptor 4 (PA-CXCR4) transmitted intracellular CXCR4 signals in response to 505-nm light. Localized activation of PA-CXCR4 induced T-cell polarization and directional migration (phototaxis) both in vitro and in vivo. Directing light onto the melanoma was sufficient to recruit PA-CXCR4–expressing tumor-targeting cytotoxic T cells and improved the efficacy of adoptive T-cell transfer immunotherapy, with a significant reduction in tumor growth in mice. These findings suggest that the use of photoactivatable chemokine receptors allows remotely controlled leukocyte trafficking with outstanding spatial resolution in tissues and may be feasible in other cell transfer therapies.

CD8 | tumor immunology | chemotaxis | multiphoton microscopy

The chemokine family performs a central function in leukocyte migration because it includes major players in the determination of tissue-specificity and selectivity during leukocyte recruitment. A number of fundamental pathophysiological processes are dependent on chemokine-mediated cell migration, including inflammation and cancer metastasis. However, therapies aimed at controlling cell migration by manipulating specific chemokine signals have been limited.

T-cell–based immunotherapy has emerged as a powerful treatment option for several disease conditions, including patients with unresectable stage III and IV metastatic melanoma (1). The efficacy of adoptive cell transfer (ACT) in cancer immunotherapy and clinical response rates are strongly correlated to the number of adoptively transferred T cells that infiltrate the tumor microenvironment (2), but the trafficking efficiency of transferred T cells is extremely low (3, 4). Although the intratumoral delivery of a chemokine-encoding system has been proposed to enhance cytotoxic T cell (CTL) homing to the tumor site (5), chemokines directly contribute to tumor growth, metastasis, and angiogenesis (6). Thus, to selectively and precisely control chemokine signal and migration of T cells in vivo, we developed a photoactivatable chemokine receptor that transmits intracellular chemokine signals and guides cell migration both in vitro and in vivo in response to localized stimulation with a specific wavelength of light.

Results

Engineering of Photoactivatable Chemokine C-X-C Motif Receptor 4. To enable the phototactic migration of T cells, we took advantage of the shared structure–function relationships of G protein coupled receptors (GPCRs) to develop and express a rhodopsin-chemokine receptor chimera with a transduction mechanism that couples an extracellular optical signal to intracellular chemokine effector functions. Based on previously published structural models (7, 8), photoactivatable chemokine receptor CXCR4 (PA-CXCR4) chimera was carefully designed to swap the G protein functions of rhodopsin-coupled $G\alpha_t$ with CXCR4-associated $G\alpha_i$ and to optimize surface expression in mammalian cells (Fig. 1 *A* and *C*). The $t_{1/2}$ value of rhodopsin chromophore formation (*A*500) is 2.7 min with 3.3 μM 11-*cis*-retinal (9), and both human blood and mouse blood contain ∼1 μM retinol (10, 11), enabling the use of the opsin-receptor chimera as a new class of in vivo immunological tools that does not require supplementation with exogenous retinal cofactors.

A 3D model for the retinal-bound PA-CXCR4 structure revealed no major rearrangement in the retinal-binding pocket compared with WT rhodopsin (Fig. S1) (12, 13). This finding suggests that the transmembrane domains of PA-CXCR4, which originated from rhodopsin, compensate for the structural and mechanical stresses resulting from the chimeric design and that the bulky side chains around retinal are not significantly affected by the CXCR4 cytoplasmic domains. Transient transfections of PA-CXCR4-mCherry into human and mouse T cells further confirmed the successful expression of the construct at the plasma membrane (Fig. 1*B* and Fig. S2).

Optical Control of Chemokine Receptor Signal Transduction. One of the earliest events after chemokine stimulation is a transient increase in the intracellular Ca^{2+} concentration ($[Ca^{2+}]_i$). To test

Significance

Precise regulation of chemokine signal is critical for directional migration of cells. In the study of complex cell behavior, it remains difficult to manipulate chemokine activity at precise times and places within living animals, and it is not possible to study different chemokine effects on defined cell types over a range of timescales. Furthermore, a given chemokine can activate multiple chemokine receptors and vice versa. Here we developed a photoactivatable chemokine receptor that can induce highly specific chemokine signals and guide cell migration toward the light stimulation. This work will advance our understanding of the cell migration process with a number of previously unidentified findings. Clinically, our photoactivatable chemokine receptor approach may have broad applications for adoptive cell transfer therapy.

Author contributions: Y.X., Y.-M.H., S.A.G., E.M.L., and M.K. designed research; Y.X., Y.-M.H., K.L., H.L., R.J.C., S.A.G., and S.B. performed research; T.Y.C. and E.M.L. contributed new reagents/analytic tools; Y.X., Y.-M.H., K.L., T.Y.C., and M.K. analyzed data; and Y.X., Y.-M.H., and M.K. wrote the paper.

The authors declare no conflict of interest.

This article is a PNAS Direct Submission. J.G.C. is a guest editor invited by the Editorial Board.

[1]Y.X. and Y.-M.H. contributed equally to this work.

[2]To whom correspondence should be addressed. E-mail: Minsoo_Kim@urmc.rochester.edu.

This article contains supporting information online at www.pnas.org/lookup/suppl/doi:10.1073/pnas.1319296111/-/DCSupplemental.

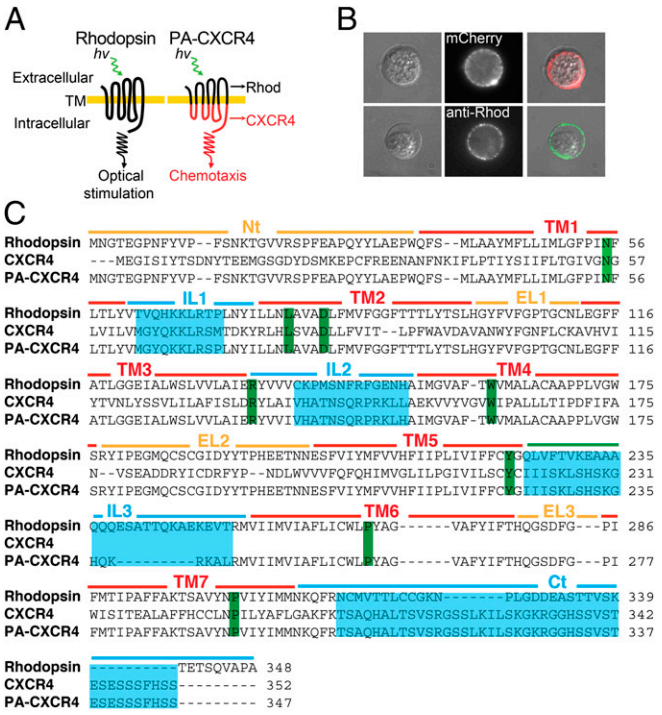

Fig. 1. Engineering of photoactivatable CXCR4 (PA-CXCR4). (*A*) PA-CXCR4 design. Rhod, rhodopsin. (*B*) Expression of PA-CXCR4-mCherry in human primary T cells. (*C*) Primary structure alignment of WT rhodopsin, WT CXCR4, and PA-CXCR4. Green, highly conserved residues; cyan, swapped intracellular domains (Nt, N terminus; TM, transmembrane domain; IL, intracellular loop; EL, extracellular loop; Ct, C terminus).

the functional responses of PA-CXCR4, we imaged $[Ca^{2+}]_i$ in mouse T cells transfected with PA-CXCR4. Fluorescence imaging of $[Ca^{2+}]_i$ demonstrated that stimulation with green light (488 ± 10 nm, 4.00 mW) was sufficient to drive prominent downstream $[Ca^{2+}]_i$ signals in PA-CXCR4–expressing cells but not in wild-type control cells (WT CXCR4), indicating the functional expression of PA-CXCR4 (Fig. 2*A*, Movie S1, and Fig. S3). CXCL12 binds to CXCR4 and activates G protein-mediated signaling through the $G\alpha_i$ pathway, which reduces cyclic adenosine monophosphate (cAMP) levels within cells. To further test the specific chemokine signals controlled by PA-CXCR4, HEK293 cells (Fig. 2*B*) or mouse T cells (Fig. 2*C*) expressing WT CXCR4 or PA-CXCR4 were stimulated with forskolin, and decreases in forskolin-induced cAMP production were then measured after CXCL12 treatment (for WT CXCR4) or excitation with 505-nm light (for PA-CXCR4). Optical stimulation yielded a significant decrease in forskolin-induced cAMP production comparable to that achieved by CXCL12 stimulation of WT CXCR4 (Fig. 2 *B* and *C*). The cells remained nonresponsive when illuminated with wavelengths longer than rhodopsin absorbance (535 or 635 nm) (Fig. 2*C*). We also observed protein kinase Akt and serine/threonine-protein kinase PAK1 activation (phosphorylation), which are parts of another canonical CXCR4 signaling pathway that is critical for CXCL12-mediated cell migration. The phosphorylation of Akt and PAK1 peaked between 3 and 20 min following light stimulation of PA-CXCR4–expressing mouse T cells. The trend was similar to what was observed in WT cells treated with CXCL12 (Fig. 2*D*). CXCR4 can also stimulate Rho kinase and phosphorylate myosin light chain (MLC) through the $G\alpha_{12/13}$ pathway (14). The phosphorylation of MLC was observed following light stimulation of PA-CXCR4–exrepssing HEK293 cells, similar to what was shown in WT CXCR4-expressing cells treated with CXCL12 (Fig. S4). However, optical stimulation of blue opsin-expressing cells failed to induce significant phosphorylation of MLC, suggesting that unlike PA-CXCR4, light-induced activation of blue opsin GPCR signals is not mediated by $G\alpha_{12/13}$ (15). Important functions of CXCR4 critically depend on its cell surface expression, which is regulated by receptor endocytosis, intracellular trafficking, and recycling. Treatment of T cells with CXCL12 induced the endocytosis of surface WT CXCR4 (receptor desensitization), which was reversed by removing the extracellular CXCL12 (Fig. S5). Consistently, illumination of

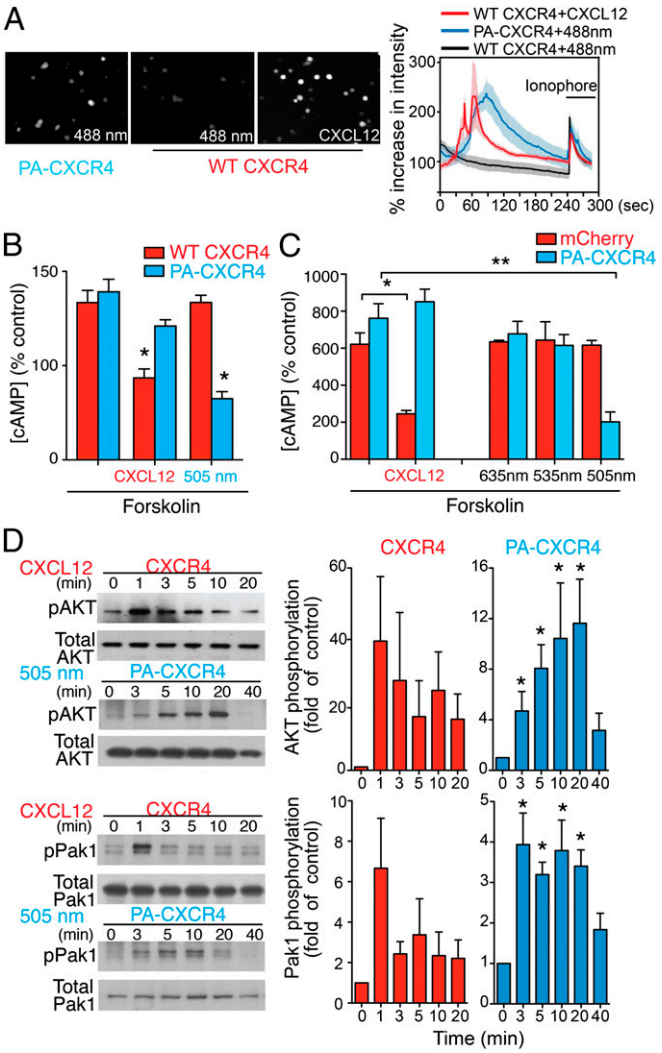

Fig. 2. Characterization of PA-CXCR4. (*A*) Fluo-4 Ca^{2+} imaging. Intensity traces of mouse OT-I CD8 T cells (WT CXCR4) and cells transiently transfected with PA-CXCR4-mCherry (PA-CXCR4). The cells were stimulated with CXCL12 or 488-nm light, followed by a Ca^{2+} ionophore. For the PA-CXCR4–expressing cells, the Ca^{2+} traces were measured only in positive transfectants (white circles; Movie S1). PA-CXCR4, $n = 5$; WT CXCR4, $n = 32$. Mean ± SEM. (*B*) The inhibition of forskolin-induced cAMP production in HEK 293 cells. $^*P < 0.05$ compared with forskolin alone (mean ± SEM, $n = 3$). (*C*) The inhibition of forskolin-induced cAMP production in mouse T cells expressing mCherry or PA-CXCR4-mCherry (PA-CXCR4). Optical stimulations were performed with indicated wavelengths. $^*P < 0.05$ compared with forskolin alone (mean ± SEM, $n = 3$). (*D*) Immunoblots from mouse OT-I CD8 T cells (CXCR4) and cells transiently transfected with PA-CXCR4-mCherry (PA-CXCR4) were probed for phosphorylated (pAkt; pThr308, and pPAK1) and total Akt and PAK1. Densitometric analysis of pAkt and pPAK1 were normalized to total protein levels and expressed as mean fold increase compared with control (time = 0 min). Data are expressed as mean ± SEM from three independent experiments. $^*P < 0.05$.

PA-CXCR4 expressing T cells with 505-nm light decreased the cell surface levels of PA-CXCR4, whereas removal of the light stimulation restored the surface expression (Fig. S5).

Activation of PA-CXCR4 Induces T-Cell Polarization and Migration in Vitro. We next used PA-CXCR4 to determine if localized chemokine activation is sufficient to induce T-cell polarization. Mouse T cells expressing GFP remained quiescent when illuminated with 505-nm light (Fig. S6 and Movie S2). In contrast, the repeated illumination of PA-CXCR4–expressing T cells led first to lamellipodial protrusions and membrane ruffles around the cell edges and then to complete cell polarization (Fig. 3*A* and Movie S3). To determine the specific effects of PA-CXCR4 on T-cell polarization, kymographs were used to quantify the maximum protrusion length. Illumination of PA-CXCR4 elicited membrane protrusions that were significantly longer than those observed in the cells expressing GFP (Fig. 3*B*). Most of the light-induced lamellipodial generations in PA-CXCR4–expressing cells occurred in the near-perpendicular direction (angles between ±45°) relative to the point of illumination, whereas the spontaneous membrane protrusions were formed in random directions in GFP-expressing T cells (Fig. 3*B*). Rap1, a member of the Ras family of small GTPases, modulates T-cell polarization and integrin activation during migration (16). A Rap1 Raichu fluorescence resonance energy transfer (FRET) sensor (17) revealed that the stimulation of CXCR4 signals in a spatially confined area of the cell led to rapid, localized Rap1 activation that did not readily spread outward from the illuminated spot (Fig. 3*C* and Movie S4). Therefore, Rap1 activation appears to be compartmentalized near chemokine signals, suggesting a polarized distribution of Rap1 activation toward a chemokine gradient during cell migration. Pretreatment of the cells with pertussis toxin (PTX) completely abolished PA-CXCR4–induced Rap1 activation (Movie S5).

The primary function of chemokine receptor is to guide directional cell migration toward a chemokine concentration gradient. The ability of PA-CXCR4 to control the directional migration of T cells was first confirmed by repeated illumination at the cell edge, which produced prolonged cell movement by generating a consistent, coordinated extension of the leading edge and retraction of the uropod (Fig. 3*D*, *i*, and Movie S6). Moving the spot of illumination to the uropod position led to the cessation of cell migration to the previous illumination position, with new polarized activities appearing where the light spot was placed (Fig. 3*D*, *ii*, and Movie S6), demonstrating reversible cell polarization by light stimulation. We then examined whether the activation of PA-CXCR4 at the posterior end of a migrating T cell can break the preexisting cell polarization and reorient the migration (Fig. 3*D*, *iii*). Aiming optical stimulation at the tail of a migrating T cell resulted in new, synchronized lamellipodial initiation at the back and rapid retraction at the original front, followed by cell movement in the reverse direction using the newly created leading edge (Fig. 3*D*, *iii*, and Movie S7).

In response to external chemokine gradients, chemokine receptors generate persistent local excitatory signals to guide directional cell migration (18). Therefore, in contrast to other photoactivatable proteins, which require light stimulation at or proximity to the cell membrane to induce cell migration (15, 19), an important advantage of PA-CXCR4 is its ability to recruit cells over a long distance toward a light gradient in a way similar to cell migration along a chemokine gradient. We demonstrated this by placing diffracted illumination at the center of the cell migration plate. The illumination of 20-μm or 100-μm spots on the plate successfully recruited PA-CXCR4–expressing T cells toward the light gradients, suggesting that the activation of PA-CXCR4 induces phototaxis (chemotaxis toward a light gradient) (Fig. 3*D*, *iv*, and Movies S8 and S9). These results, in combination with the earlier biochemical data in Fig. 2, support the conclusion that PA-CXCR4 can be functionally expressed in T cells to permit the photoactivatable control of chemotactic signals and to modulate directional cell migration using light.

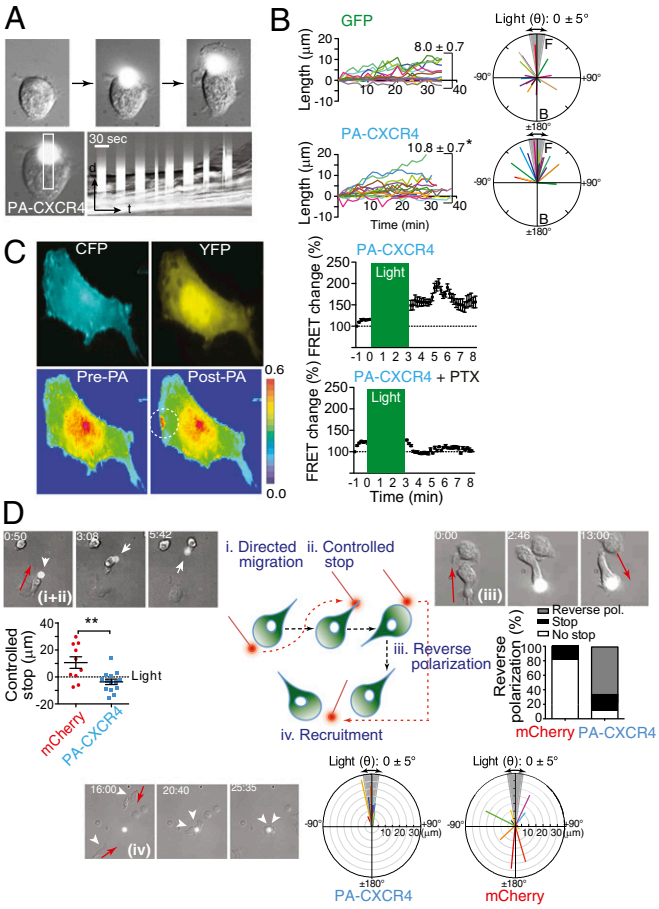

Fig. 3. Activation of PA-CXCR4 induces T-cell polarization and migration in vitro. (*A*) Repeated illumination of a mouse CD4$^+$ T cell expressing PA-CXCR4 induced cell membrane protrusions and polarization. A narrow rectangular region of interest was obtained from each image in the time lapse series and then pasted in a montage to form the kymograph picture (*Lower Right*). (*B*) The average angle of cell polarization (*Right*; the angle of the illumination spot was 0 ± 5° to the cell centroid) and cell length (distance between cell centroid and membrane protrusion; *Left*; mean ± SEM; $*P < 0.05$ compared with GFP) are shown. (*C*) GD25 cells were transiently transfected with Rap1 FRET sensor and PA-CXCR4 and illuminated in a 10-μm circle (white) with 505-nm light for 3–5 min. FRET efficiencies before (pre) and after (post) light stimulation are shown in rainbow colors, from high (red) to low (blue). Results from five individual experiments were normalized according to the basal energy transfer. (*D*) Schematic of in vitro T-cell migration test with light stimulation (*Center*). In the images labeled *I* and *ii*, the repeated illumination at the edge of mouse CD4 T cells transiently expressing PA-CXCR4 (white arrow) induced directional migration on ICAM-1–coated surface (directed migration), and T cells stopped upon light activation at the uropod (controlled stop). T-cell migration after controlled stop was quantified (mean ± SEM; $**P < 0.01$). In the images labeled *iii*, reverse polarization was induced by continuous illumination at the uropod of PA-CXCR4–expressing mouse CD4 T cells. The percentages of stop and reverse polarization were quantified (mCherry-expressing T cells, $n = 10$; PA-CXCR4–expressing T cells, $n = 14$). In the images labeled *iv*, T cells expressing PA-CXCR4-mCherry migrated toward the area of light illumination (phototaxis) (arrowhead). Light mediated directional T-cell migration was quantified (mCherry, $n = 23$; PA-CXCR4, $n = 12$). Red arrow, direction of cell migration.

Optical Control of T-Cell Recruitment in Vivo. The first response of rolling and tethering T cells to local chemokine stimulation in vivo is rapid integrin activation and firm adhesion to the blood

vessel wall, which is followed by crawling and transendothelial migration. The light-mediated rapid, firm adhesion of PA-CXCR4–expressing T cells was confirmed in vivo. T cells were arrested in the femoral vein triggered by local optical stimulation with 0.48 mW/mm^2 light at 488 ± 10 nm (Fig. 4 and Movies S10 and S11). Within seconds of ending the light stimulation, many adherent T cells quickly detached from the blood vessel, demonstrating the reversibility of the light-mediated activation of chemokine signals in vivo (Fig. 4 and Movie S10).

In a long-term in vivo T-cell recruitment assay, we attached a 200-μm cyan light-emitting diode (LED; 25 mW at 505 ± 15 nm) optical fiber onto the hairless area of an unshaven mouse ear (Figs. S7 and S8). The directional guidance of cell migration requires chemotactic molecule gradients, with at least 2% differences in concentration between the front and back of a cell (18). To determine whether a stable light gradient was established in the ear dermis by the optical fiber to guide T-cell extravasation and migration, we first measured the light propagation pattern in the mouse ear (Fig. S8*A*). The light–power density profiles revealed the gradual attenuation of light intensity in the mouse ear, both vertically (*z* direction; Fig. S8*B*) and horizontally (*x*–*y* direction; Fig. S8*C*). The computed average vertical light intensity delta corresponded to a 2% decrease every 10 μm (approximately one mouse T-cell diameter). This result suggests that our in vivo optical stimulation can successfully deliver a functionally active light gradient for directional T-cell migration in the dermis.

Using this system, we performed homing assays to assess the ability of local optical stimulation to regulate chemotactic signals in PA-CXCR4 cells and to guide cell migration in vivo. In vitro-activated DO.11 CD4 T cells were transfected with PA-CXCR4 ($T_{PA\text{-}CXCR4}$ cells) and then transferred into recipient mice. Cells were harvested from freely moving mice following 24, 48, or 72 h with/without light stimulation. The ratio of $T_{PA\text{-}CXCR4}$ cells in light:dark inflamed ears (OVA + CFA), spleens, and lymph nodes (LNs) was assessed. $T_{PA\text{-}CXCR4}$ cells exhibited enhanced homing to light-activated inflamed ears at 48 and 72 h, whereas homing to the spleen and LNs was not altered (Fig. 5 *A* and *C*). Conversely, the expression of control vector GFP did not lead to enhanced CD4 T-cell homing to the light-stimulated ears (Fig. 5*B*). These data suggest that local light stimulation can successfully recruit adoptively transferred PA-CXCR4–expressing T cells to targeted tissue in vivo.

Optogenetically Engineered T Cells for Cancer Immunotherapy. To demonstrate the clinical implications of PA-chemokine receptors, we examined the ability of PA-CXCR4 to enhance the efficient trafficking of adoptively transferred tumor-specific CD8$^+$ T cells toward a tumor site and to improve antigen-specific tumor regression. C57BL/6 mice were injected intradermally in the ear with B16/OVA tumor cells, which developed solid tumors that failed to be rejected in the absence of additional manipulation

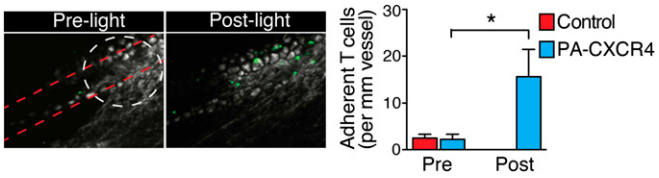

Fig. 4. In vivo T-cell firm adhesion. The firm adhesion of T cells induced by light stimulation of PA-CXCR4 was visualized in the femoral veins using two-photon intravital microscopy. Representative images of CFSA-labeled CD4$^+$ T-cell adhesion before (pre) and after (post) light stimulation (*Left*) are shown, and the number of adherent cells was measured in three independent experiments (mean ± SEM; *P < 0.05 compared with GFP-expressing control T cells).

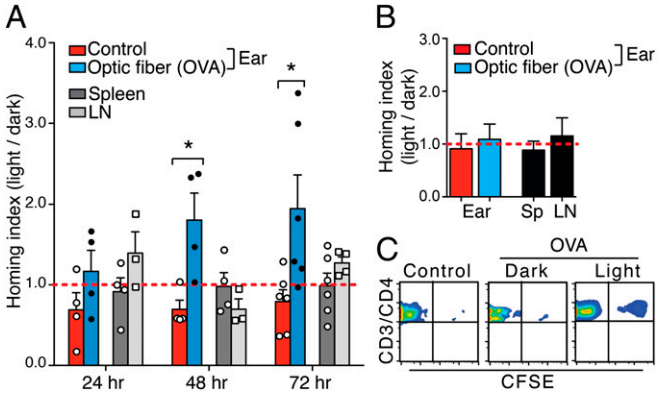

Fig. 5. In vivo T-cell recruitment. (*A*) The fold change in the T-cell homing index, as determined by the light mouse [PA-CXCR4$^+$CD4$^+$/PA-CXCR4$^-$CD4$^+$]/dark mouse [PA-CXCR4$^+$CD4$^+$/PA-CXCR4$^-$CD4$^+$] ratio. BALB/c mice were infected in one ear with $OVA_{323–339}$ peptide emulsified with CFA and subjected to light activation through an optical fiber, whereas the other ear (control) was left uninflamed without the optical fiber attached. The horizontal line (red) indicates a homing index of 1. n = 3 (mean ± SEM; *P < 0.05 compared with control). LN, cervical lymph node. (*B*) Homing index of GFP-expressing DO.11 CD4$^+$ T cells. n = 3 (mean ± SEM). (*C*) Flow cytometry analysis of transferred cells (CFSE$^+$) in an OVA/CFA-inflamed ear with (light) or without (dark) light stimulation for 72 h.

(Fig. 6*A*). Similar tumor growth patterns were observed following the transfer of 1 × 10^5 in vitro-activated OT-I CTLs. Adoptive T-cell therapy through the transfer of 1 × 10^6 OT-I CTLs resulted in a slight tumor regression but no tumor cell elimination (Fig. 6*A*). The transfer of 10 times more OT-I CTLs (1 × 10^7) failed to induce any detectable changes in tumor regression (Fig. 6*A*). This finding suggests the presence of a tumor microenvironment that suppresses the accumulation of antitumor immune responses by transferred CTLs (Fig. 6*A*) (3). Next, we transfected in vitro-activated OT-I CTLs with PA-CXCR4 and transferred the resulting PA-CXCR4$^+$CD45.1$^+$CD8$^+$ OT-I CTLs into B16/OVA tumor-bearing mice 7 d after tumor cell injection. Subsequently, the visible and palpable tumor area was illuminated with a cyan optical fiber (505 nm, 3.67 mW/mm^2) for 7 d, and tumor growth was measured for an additional 7 d without illumination. Dark mice were treated equally for a total of 21 d without light stimulation (Fig. 6*B*). Localized light stimulation for 7 d dramatically decreased tumor growth in the mouse ear (Fig. 6 *C* and *D*). Light stimulation of the mice that received GFP-transfected OT-I CTLs did not alter tumor growth, implying that the effect of 505-nm LED light alone is not detrimental to the tumor cells (Fig. 6*E*). Microscopic analyses of B16/OVA tumors confirmed that local light stimulation resulted in a marked increase in intratumoral OT-I CTL infiltration, whereas the total CD8$^+$ T-cell numbers were similar between the dark and light mice (Fig. 6 *G* and *H*). At 7 d after the PA-CXCR4$^+$CD45.1$^+$CD8$^+$ OT-I CTLs were transferred, these cells (CD45.1$^+$) accumulated in multiple discrete areas both in the periphery and in the core of the B16/OVA tumors in the presence of light stimulation, without any noticeable changes in the vascular density (Fig. 6 *F* and *I* and Movie S12). In contrast, PA-CXCR4$^+$ CTLs were mainly found in the periphery near the tumor microvessels, their likely port of entry, under the dark condition (Fig. 6 *F* and *I* and Movie S13). Our data suggest that light stimulation of PA-CXCR4 increases not only the total number of adoptively transferred CTLs but also the homing of T cells, both in the tumor center and at the periphery, and thus their local cytolytic reactions.

To further confirm that the change in tumor size was mainly due to enhanced CTL infiltration and not to the recruitment of innate effector cells, we measured other leukocyte subtypes

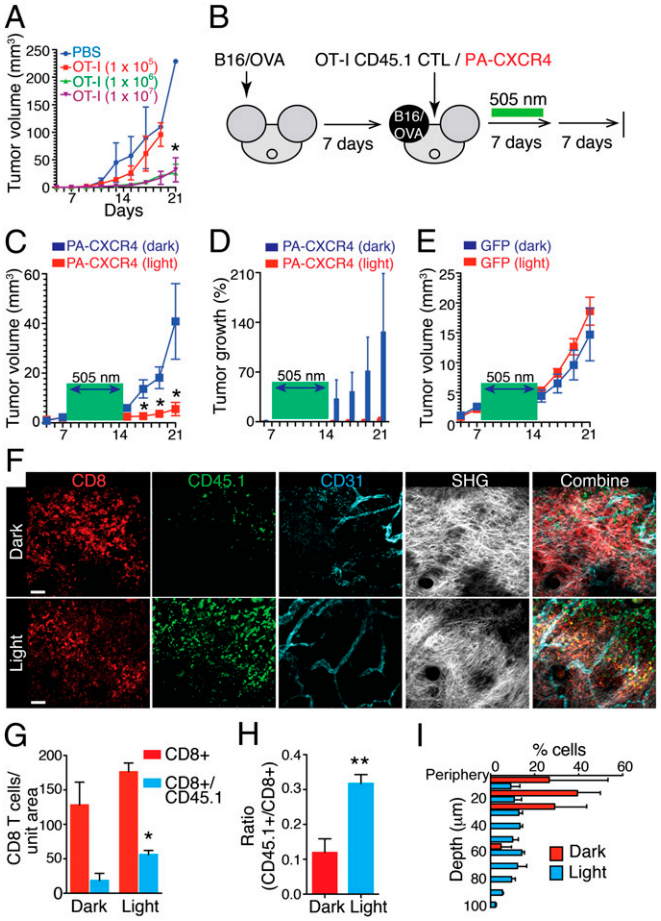

Fig. 6. Optical control of CTL migration in antitumor immunotherapy. (*A*) Antigen-specific tumor regression upon adoptive transfer of in vitro-primed CTLs. (*B*) Experimental design of the studies of the optical control of CTL migration. (*C*) Growth curves of B16/OVA tumors in mice treated with ACT of PA-CXCR4–expressing OT-I $CD8^+$ T cells with (optical fiber + light) or without (optical fiber + dark) light stimulation. The light stimulation (505-nm) times are denoted with a green box. $n = 5$ mice per condition (mean ± SEM; $^*P <$ 0.01 compared with dark). (*D*) The percent change in tumor volume (compared with day 7). (*E*) Growth curves of B16/OVA tumors in mice treated with ACT of GFP-expressing OT-I $CD8^+$ T cells with (optical fiber + light) or without (optical fiber + dark) light stimulation. $n = 5$ mice per condition (mean ± SEM). (*F*) Representative immunofluorescence images of B16/OVA tumors in mice treated with the ACT of PA-CXCR4–expressing OT-I $CD8^+$ T cells with (light) or without (dark) light stimulation (on day 14). The data are representative of more than three independent imaging experiments. (*G* and *H*) Quantification of total PA-CXCR4–expressing CTLs ($CD45.1^+$) compared with the total $CD8^+$ T-cell numbers in B16/OVA tumors by microscopy. $n = 3$ (mean ± SEM; $^*P < 0.01$ compared with dark). (*I*) $CD45.1^+$ cell location throughout the depth of the tumor.

in B16/OVA tumors. Light stimulation did not alter the number of tumor-infiltrating NK cells ($CD3^-NK1.1^+$), macrophages ($CD3^-NK1.1^-CD4^-CD8^-CD11b^+Ly6C^-Ly6G^-$), polymorphonuclear myeloid-derived suppressor cells (MDSCs) ($CD3^-NK1.1^-CD4^-CD8^-CD11b^+Ly6G^+Ly6C^{mid}$), or monocytic MDSCs ($CD3^-NK1.1^-CD4^-CD8^-CD11b^+Ly6G^-Ly6C^{hi}$) (Fig. S9 *A* and *B*). The effects of light activation of PA-CXCR4 on the quality of infiltrated CTLs were then analyzed by real-time PCR (Fig. S10). The levels of major inflammatory cytokines, including IL2 and IFN-γ, T-cell proliferation, and effector molecules, such as granzyme B and perforin, were substantially increased in the adoptively transferred CTLs after light stimulation (Fig. S10), suggesting that the enhanced trafficking of PA-CXCR4$^+$ CTLs by light stimulation can improve the quality of T-cell responses by promoting local effector functions and antitumor activity.

Discussion

Efficient migration of newly transferred cells to targeted tissues is the most critical step for achieving optimal outcomes in the ACT therapy. For example, monitoring of transferred CTLs after ACT has shown that most infused $CD8^+$ T cells localize to the lung, liver, or spleen, whereas only ∼1% of the total transferred T cells migrate to the tumor (3, 20). In addition, the majority of adoptively transferred $CD8^+$ T cells are preferentially found in the tumor periphery allowing time for escape mechanisms to be enacted in the central regions of the tumor (21, 22). In this study, we developed a photoactivatable chemokine receptor that leverages common structure–function relationships between two different GPCR families (rhodopsin receptor and chemokine receptor). PA-CXCR4 can recruit distinct T-cell populations in vivo by inducing migration signals in response to light, demonstrating that a highly selective localized chemokine signal is sufficient to recruit transferred cells to the targeted tumor in vivo and thereby elicit effective tumor rejection. Consistent with our findings, activation of endogenous G protein pathway using blue opsin resulted in similar cell migration in neutrophil by light stimulation (15). Direct illumination on the blue opsin-expressing cell surface was sufficient to generate a diffusible gradient of intracellular signaling molecules, such as phosphatidylinositol (3,4,5)-triphosphate.

Many types of tumors can actively prevent T-cell infiltration by modifying gene expression of adhesion molecules such as ICAM-1 and VCAM-1 in vascular endothelial cells (21) or by inducing posttranslational modification of local chemokine signals, including CCL2 (23). Our data are in agreement with several strategies that have been proposed to optimize antitumor T-cell migration by transducing highly targeted, localized chemokine signals at the tumor site. Furthermore, recent studies have demonstrated that adoptively transferred CD8 T cells are recruited to a s.c. EG7-thymoma model, yet remain in its periphery (22, 24). In the present study, stimulation of PA-CXCR4 with light increased the recruitment of adoptively transferred OT-I T cells and enabled them to migrate into the core of B16 tumors, leading to significantly enhanced tumor rejection. Because T cells were unable to improve their tumor infiltration under the dark condition and because the endogenous CD8 responses and intratumor vascular structures were unmodified, the effects of light stimulation were likely directly related to the recruitment (and positioning) of the transferred T cells.

Our photoactivatable chemokine receptor provides a unique opportunity to investigate the dynamic changes in polarized intracellular biochemical signals that mediate accurate lymphocyte chemotaxis, as light could be delivered to a very small and well-defined area in precisely timed pulses, and may enable optical control of other chemokine receptors with similarly designed constructs. However, it is important to note that for individual PA-chemokine receptors, it may not be possible to control of all of the receptor conformational states that are necessary to generate signals identical to those induced by the WT receptor–ligand interaction. Indeed, the trend of receptor signals (including calcium concentration and up-regulation of both pAkt and pPAK1) was similar for both CXCL12 and light stimulations in WT and PA-CXCR4 T cells, but the peak response was delayed in PA-CXCR4–expressing cells, suggesting distinct signaling kinetics. Dimerization or oligomerization of GPCR is a recognized mode of regulation of receptor activities and signaling functions. CXCR4 has been previously shown to homodimerize and heterodimerize, constitutively and upon ligand binding (25, 26). Unlike other GPCR dimerization, which depends on contacts throughout the transmembrane (TM) bundle, CXCR4 monomers interact only at the extracellular side of helices V and

VI (7). Although the biological function of CXCR4 dimerization remains incompletely characterized, a considerable body of data suggests important in vivo effects (25-27). The extracellular and the TM domains in PA-CXCR4 were originated from rhodopsin and thus may not support the specific receptor dimerization seen in WT CXCR4. Therefore, it is possible that lack of the receptor–receptor interactions may result in delayed signaling responses seen in some of our assays, although we cannot discount the possibility that new modes of dimerization may exist in PA-CXCR4, which may cause different signaling kinetics.

In vivo, different chemokines may cooperate temporally and spatially to control the movement of T cells and to prioritize their responses to the different chemokines present in the inflamed tissues. Once T cells recognize a certain pair of chemokine signals (including the PA-CXCR4 signal) at the tissue site, they can respond specifically, even overcoming an opposing chemokine gradient coming from the other vasculatures. Some chemokine receptors may become sensitized or desensitized by the interactions, allowing a certain group of chemokine receptors to dictate the T-cell migration. Alternatively, a hierarchical response may take place in a sequential manner, in which PA-CXCR4 initially dominates over other end-target chemokine signals so that T cells move along a light gradient; this signal is then ignored (or desensitized), and the T cells follow a new gradient of local chemokine receptor ligands, thus gaining access to a precise tissue site. The synergistic interactions between different chemokine receptors may not only affect T-cell migration, but it is also possible that certain types of chemokines work collaboratively to mediate T-cell retention at the tissue. Additionally, emerging evidence indicates that CXCR4 concurrently provides multiple signals to induce migration while simultaneously preparing the cell for its destination, the site where this chemokine drives T-cell development and cytokine secretion and regulates cell apoptosis (28, 29). Therefore, it is possible that an increase in the T-cell number at a tissue site following the local light stimulation of PA-CXCR4 may result from the integration of multiple outcomes of CXCR4 signaling in vivo. The levels of certain inflammatory cytokines and effector molecules were significantly increased in the adoptively transferred T cells after light stimulation, suggesting additional effects of PA-CXCR4 on the quality and magnitude of the T-cell response.

Materials and Methods

To apply light illumination to mouse T cells in vivo, a Nikon Eclipse TE2000-E microscope (Nikon) was equipped with Mosaic microelectromechanical systems (MEMS) Digital Mirror Device (Andor Technology). PA-CXCR4-mCherry–expressing mouse T cells and GFP-expressing mouse T cells were generated using a retroviral expression system, as described above. The cells were then resuspended in L15 medium (Gibco) containing 2 mg/mL glucose (Sigma) at 4 °C and placed on a mouse ICAM-1–coated Delta T dish (Bioptechs). The cell edge was activated using light (505 nm, 2-μm diameter) in a 30-s light/30-s dark cycle. Time lapse images were acquired at room temperature or at 37 °C. Image acquisition and analysis were performed using NIS-Element software (Nikon). Detailed methods may be found in *SI Materials and Methods*.

ACKNOWLEDGMENTS. The authors thank Jennifer Wong, Jim Miller, Christina Baker, Hung-Li Chung, and Nathan Laniewski for reagents and for technical assistance and the M.K. laboratories for discussion and support. This work was supported by National Institutes of Health (NIH) Grant HL018208, NIH Grant HL087088, and World Class University Grant R32-10084 (to M.K.); NIH Grant CA28332 (to E.M.L.); and American Heart Association Grant 11SDG7520018 (to Y.-M.H.).

1. Lizée G, et al. (2013) Harnessing the power of the immune system to target cancer. *Annu Rev Med* 64:71–90.
2. Fridman WH, Pagès F, Sautès-Fridman C, Galon J (2012) The immune contexture in human tumours: Impact on clinical outcome. *Nat Rev Cancer* 12(4):298–306.
3. Fisher B, et al. (1989) Tumor localization of adoptively transferred indium-111 labeled tumor infiltrating lymphocytes in patients with metastatic melanoma. *J Clin Oncol* 7(2):250–261.
4. Griffith KD, et al. (1989) In vivo distribution of adoptively transferred indium-111-labeled tumor infiltrating lymphocytes and peripheral blood lymphocytes in patients with metastatic melanoma. *J Natl Cancer Inst* 81(22):1709–1717.
5. Gao JQ, Okada N, Mayumi T, Nakagawa S (2008) Immune cell recruitment and cell-based system for cancer therapy. *Pharm Res* 25(4):752–768.
6. Kang H, et al. (2005) Stromal cell derived factor-1: Its influence on invasiveness and migration of breast cancer cells in vitro, and its association with prognosis and survival in human breast cancer. *Breast Cancer Res* 7(4):R402–R410.
7. Wu B, et al. (2010) Structures of the CXCR4 chemokine GPCR with small-molecule and cyclic peptide antagonists. *Science* 330(6007):1066–1071.
8. Hofmann KP, et al. (2009) A G protein-coupled receptor at work: The rhodopsin model. *Trends Biochem Sci* 34(11):540–552.
9. Reeves PJ, Hwa J, Khorana HG (1999) Structure and function in rhodopsin: Kinetic studies of retinal binding to purified opsin mutants in defined phospholipid-detergent mixtures serve as probes of the retinal binding pocket. *Proc Natl Acad Sci USA* 96(5):1927–1931.
10. O'Byrne SM, et al. (2005) Retinoid absorption and storage is impaired in mice lacking lecithin:retinol acyltransferase (LRAT). *J Biol Chem* 280(42):35647–35657.
11. Faure H, et al. (2006) Factors influencing blood concentration of retinol, alpha-tocopherol, vitamin C, and beta-carotene in the French participants of the SU.VI. MAX trial. *Eur J Clin Nutr* 60(6):706–717.
12. Park PS, Lodowski DT, Palczewski K (2008) Activation of G protein-coupled receptors: Beyond two-state models and tertiary conformational changes. *Annu Rev Pharmacol Toxicol* 48:107–141.
13. Palczewski K, et al. (2000) Crystal structure of rhodopsin: A G protein-coupled receptor. *Science* 289(5480):739–745.
14. Tan W, Martin D, Gutkind JS (2006) The Galpha13-Rho signaling axis is required for SDF-1-induced migration through CXCR4. *J Biol Chem* 281(51):39542–39549.
15. Karunarathne WK, Giri L, Patel AK, Venkatesh KV, Gautam N (2013) Optical control demonstrates switch-like PIP3 dynamics underlying the initiation of immune cell migration. *Proc Natl Acad Sci USA* 110(17):E1575–E1583.
16. Shimonaka M, et al. (2003) Rap1 translates chemokine signals to integrin activation, cell polarization, and motility across vascular endothelium under flow. *J Cell Biol* 161(2):417–427.
17. Mochizuki N, et al. (2001) Spatio-temporal images of growth-factor-induced activation of Ras and Rap1. *Nature* 411(6841):1065–1068.
18. Iglesias PA, Devreotes PN (2008) Navigating through models of chemotaxis. *Curr Opin Cell Biol* 20(1):35–40.
19. Wu YI, et al. (2009) A genetically encoded photoactivatable Rac controls the motility of living cells. *Nature* 461(7260):104–108.
20. Bobisse S, et al. (2009) Reprogramming T lymphocytes for melanoma adoptive immunotherapy by T-cell receptor gene transfer with lentiviral vectors. *Cancer Res* 69(24):9385–9394.
21. Fisher DT, et al. (2011) IL-6 trans-signaling licenses mouse and human tumor microvascular gateways for trafficking of cytotoxic T cells. *J Clin Invest* 121(10):3846–3859.
22. Boissonnas A, Fetler L, Zeelenberg IS, Hugues S, Amigorena S (2007) In vivo imaging of cytotoxic T cell infiltration and elimination of a solid tumor. *J Exp Med* 204(2):345–356.
23. Molon B, et al. (2011) Chemokine nitration prevents intratumoral infiltration of antigen-specific T cells. *J Exp Med* 208(10):1949–1962.
24. Breart B, Lemaître F, Celli S, Bousso P (2008) Two-photon imaging of intratumoral CD8+ T cell cytotoxic activity during adoptive T cell therapy in mice. *J Clin Invest* 118(4):1390–1397.
25. Babcock GJ, Farzan M, Sodroski J (2003) Ligand-independent dimerization of CXCR4, a principal HIV-1 coreceptor. *J Biol Chem* 278(5):3378–3385.
26. Wang J, He L, Combs CA, Roderiquez G, Norcross MA (2006) Dimerization of CXCR4 in living malignant cells: Control of cell migration by a synthetic peptide that reduces homologous CXCR4 interactions. *Mol Cancer Ther* 5(10):2474–2483.
27. Hamatake M, et al. (2009) Ligand-independent higher-order multimerization of CXCR4, a G-protein-coupled chemokine receptor involved in targeted metastasis. *Cancer Sci* 100(1):95–102.
28. Kumar A, et al. (2006) CXCR4 physically associates with the T cell receptor to signal in T cells. *Immunity* 25(2):213–224.
29. Gleimer M, von Boehmer H (2010) Thymocyte selection: Chemokine signaling is not only about the destination. *Curr Biol* 20(7):R316–R318.